

A matrix product operator approach to non-equilibrium Floquet steady states

Zihan Cheng¹ and Andrew C. Potter^{1,2}

¹*Department of Physics, University of Texas at Austin, Austin, TX 78712, USA*

²*Department of Physics and Astronomy, and Quantum Matter Institute,
University of British Columbia, Vancouver, BC, Canada V6T 1Z1*

We present a numerical method to simulate non-equilibrium Floquet steady states of one-dimensional periodically-driven (Floquet) many-body systems coupled to a dissipative bath, called open-system Floquet DMRG (OFDMRG). This method is based on a matrix product operator ansatz for the Floquet density matrix in frequency-space, and enables access to large systems beyond the reach of exact master-equation or quantum trajectory simulations, while retaining information about the periodic micro-motion in Floquet steady states. An excited-state extension of this technique also allows computation of the dynamical approach to the steady state on asymptotically long timescales. We benchmark the OFDMRG approach with a driven-dissipative Ising model, and apply it to study the possibility of dissipatively stabilizing pre-thermal discrete time-crystalline order by coupling to a cold bath.

Controlling quantum systems with time-periodic (Floquet) external driving fields offers a powerful toolkit to engineer interactions, symmetry-breaking, and topology that are not present in the un-driven system [1]. Floquet driving can also produce *intrinsically non-equilibrium* phenomena such as dynamical phases like time crystals and Floquet topological phases [2, 3], with properties that would be impossible in static equilibrium. However, for isolated systems, persistent energy absorption from external driving ordinarily produces runaway heating to a featureless state [4, 5] that is locally indistinguishable from an infinite temperature ensemble. Thus, to stabilize dynamical phases in closed Floquet systems, one usually considers systems with many-body localization [6] that fail to thermalize, or work in a pre-thermal regime [7–13] where Floquet states can live up an exponentially-long timescale $\tau_{\text{heat}} \sim e^{\Omega/\Lambda}$ in the ratio of driving frequency Ω , to the local bandwidth, Λ . Both of these approaches have substantial limitations. First, MBL requires synthesizing strong disorder, and is fundamentally incompatible with many interesting phenomena such as non-Abelian symmetries and anyons [14], Goldstone modes [15], long-range interactions and (at least as a matter of principle if not practice) in dimensions higher than one [16]. Second, no experimental system is truly isolated from its environment, which restricts MBL-protected order to transient times. Realizing pre-thermal *quantum* phases requires preparing a low-temperature state of the pre-thermal Hamiltonian which is typically hard to even calculate, let alone prepare its ground-state (e.g. adiabatic state-preparation generally fails in Floquet settings [17]).

Experience from solid-state physics, it is natural to look to dissipation from a cold bath to cool a Floquet system close to its pre-thermal ground-state. For fast, weakly-heating drives, rigorous bounds on pre-thermalization [7–13] establish a large separation of time scales between the drive period $\tau = 2\pi/\Omega$, and the heating time τ_{heat} . This suggests an ample range of parameter

space to couple the system to a bath weakly enough to avoid disrupting the interesting Floquet dynamics, while cooling towards the pre-thermal ground-state at a rate much higher than the drive-induced heating. On the other hand, coupling a system to a bath can enhance drive-induced heating, by broadening spectral lines in the system to enable off-resonant drive-induced excitations that cause the system to heat [18]. To explore the balance between these competing processes and establish whether dissipation can stabilize dynamical orders in an appropriately designed range of drive, bath, and system-bath coupling parameters, it requires a controlled calculation method that can simultaneously treat strong driving, interactions, and open system dynamics.

However, solving the long-time non-equilibrium steady state (NESS) of a generic Floquet-Lindblad equation [19–22] (FLE) is a challenging task, even for one-dimensional systems. Similar to solving Schrodinger equation, the cost of exact treatment grows exponentially with respect to the system size, but with a *double(!)* exponent due to simulating density matrices rather than pure states. Quantum trajectory sampling methods [23–25] reduce the memory cost, but may incur exponential-in-system-size sampling overheads.

In one dimension ($1d$), matrix product states (MPS) and operators (MPO) provide an effective way of representing systems with limited spatial entanglement – a class that includes not only ground-states of gapped systems [26] but also thermal mixed-states [27]. One class of MPO approaches [28–31], in combination with time-evolving block decimation (TEBD) methods, allows studying the NESS via long-time dynamics. Such real-time approaches can suffer from the long relaxation time to the NESS, for example in the presence of long-time hydrodynamic tails, and weakly-dissipative systems may also feature a rapid growth of entanglement in the transient regime that cannot be captured by a low bond-dimension MPO [32–34], presenting a short-time barrier

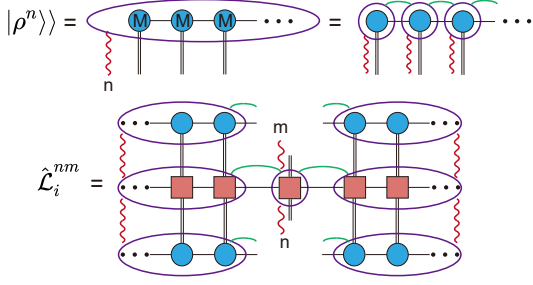


FIG. 1. **Graphical representation** – of vectorized MPOs $|\rho^n\rangle\rangle$ (upper) and effective local Lindbladian $\hat{\mathcal{L}}_i^{nm}$ (lower) in frequency-space. Blue circles and black single/double lines respectively represent the tensor and bond/physical indices in the Hilbert space, while the purple circle and red wavy lines represent the tensor and Fourier indices in frequency-space. Green lines represent the virtual bond space where each tensor is block diagonal in n .

to accessing the NESS through time-evolution.

To overcome these limitations, for time-independent systems, recent works [32, 33] directly target an MPO representation of a NESS that is variationally optimized through density matrix renormalization group (DMRG) type methods [35]. In this paper, we extend this technique to open Floquet systems. The central idea will be to reduce the time-dependent Floquet problem to an effective time-independent one in an extended (frequency) space. Frequency-space methods are widely used in various analytic and numerical approaches to Floquet problems [36]. Here we adapt this representation in a form convenient for performing MPS calculations. Importantly, the method retains information not only about the NESS at stroboscopic times, but also the micro-motion within a period, which can be required to observe certain dynamical phases, such as Floquet topological insulators and symmetry-protected topological phases [2]. We also benchmark this method with a driven-dissipative Ising model and use it to explore the dissipative stabilization of a discrete time-crystal (DTC) by coupling it to a cold bath.

Frequency-space MPO representation – Consider the evolution of the density matrix $\rho(t)$ of a periodically driven $1d$ quantum system coupled to a Markovian bath described by the Floquet-Lindblad equation (FLE):

$$\partial_t \rho = \mathcal{L}(t)[\rho] = -i[H(t), \rho] + \sum_{\alpha} \left(L_{\alpha}(t) \rho L_{\alpha}^{\dagger}(t) - \frac{1}{2} \{L_{\alpha}^{\dagger}(t) L_{\alpha}(t), \rho\} \right), \quad (1)$$

where $H(t+\tau) = H(t)$ and $L_{\alpha}(t+\tau) = L_{\alpha}(t)$ are respectively the periodic Hamiltonian and jump operators.

Floquet's theorem enables one to write solutions to the FLE in terms of quasi-eigenmodes of the Lindbladian $\mathcal{L}(t)$ as: $\rho(t) = \sum_n \rho^n e^{-\lambda t} e^{in\Omega t}$, where λ is the (complex) quasi-eigenvalue and $\Omega = 2\pi/\tau$ is the driving frequency (See Appendix A for details). Inserting this expression

into Eq. 1, reduces the time-dependent FLE into an effectively time-independent equation: $\hat{\mathcal{L}}[\hat{\rho}] = -\lambda\hat{\rho}$ for extended $\hat{\rho} = \sum_n \rho^n \otimes |n\rangle\rangle$ residing in an enlarged (frequency) space $\mathcal{H}^2 \times \mathbb{Z}$ (intuitively, the extra \mathbb{Z} factor keeps track of how many drive quanta the system has absorbed or released), where the extended Lindbladian is given by:

$$\hat{\mathcal{L}}^{nm}[\rho^m] = -in\Omega \rho^n \delta_{nm} - i[H^{n-m}, \rho^m] + \sum_{\alpha} D_{\alpha}^{nm}[\rho^m],$$

$$D_{\alpha}^{nm}[\rho^m] = L_{\alpha}^{n-k} \rho^m L_{\alpha}^{\dagger, k-m} - \frac{1}{2} \{L_{\alpha}^{\dagger, n-k} L_{\alpha}^{k-m}, \rho^m\}, \quad (2)$$

where H^n , L_{α}^n are Fourier coefficients of H and L_{α} with frequency $n\Omega$ respectively, and throughout this paper repeated Fourier indices are implicitly summed.

We are targeting models with high-frequency drives and weak-system bath couplings to model whether a system can be cooled close to a pre-thermal ground-state. Here, we expect ρ^0 to be approximately thermal, and hence exhibit an area-law operator entanglement [27] permitting efficient representation as an MPO. We further assume that, at high frequencies, the linear potential $-in\Omega$ in frequency-space leads to localization near $n=0$ characterized by rapid decay of $|\rho^n|/|\rho^0|$ with n (See Appendix B for convergence check), so that we can cut off the infinite frequency index beyond $|n| = N_c$, and that each ρ^n has a low bond-dimension MPO representation $\forall n$. The validity of assumptions can be checked *a posteriori*. We note that the Fourier index n can be regarded either as a global index, or distributed to each MPO tensor as an auxiliary label to the virtual bond space where each tensor is block diagonal in n (see Fig. 1 for a graphical representation). It is further convenient to vectorize the density matrices $\rho^n \rightarrow |\rho^n\rangle\rangle$ using the Choi isomorphism $|\psi\rangle\langle\phi| \rightarrow |\psi \otimes \phi\rangle\rangle$, so that we regard the MPO as an MPS with squared physical dimension:

$$|\rho^n\rangle\rangle = \sum_{\{\mu_i\}} M_{\mu_1}^n \dots M_{\mu_L}^n |\mu_1 \dots \mu_L\rangle\rangle, \quad (3)$$

where each M^n is a $d^2 \times \chi \times \chi$ tensor, d is the onsite Hilbert space dimension, $\mu_i \in \{1 \dots d^2\}$ labels a basis of physical states for the vectorized density matrix, $i = 1 \dots L$ label sites of the $1d$ chain, and χ is the bond dimension.

After the vectorization, $\hat{\mathcal{L}}^{nm}$ in Eq.(2) becomes a linear operator acting on $|\rho^m\rangle\rangle$, which can be similarly represented in an MPO form with two Fourier components n, m :

$$\hat{\mathcal{L}}^{nm} = \sum_{\{\mu_i, \nu_i\}} v^L W_{\mu_1 \nu_1}^{nm} \dots W_{\mu_N \nu_N}^{nm} v^R |\mu_1 \dots \mu_N\rangle\rangle \langle \nu_1 \dots \nu_N|, \quad (4)$$

where each W^{nm} is a $d^2 \times d^2 \times \chi_O \times \chi_O$ tensor, χ_O are the operator bond dimension, and $v^{L,R}$ impose boundary conditions.

Open-system Floquet DMRG (OFDMRG) – In conventional MPS-DMRG for closed systems, one minimizes the variation energy $\langle \psi | H | \psi \rangle$ for each local MPS

tensor, which relies heavily on Hermiticity of H . A natural generalization [32] to open systems would be to minimize $\langle\langle \rho | \mathcal{L}^\dagger \mathcal{L} | \rho \rangle\rangle$, however, the MPO for $\mathcal{L}^\dagger \mathcal{L}$ has square of the bond-dimension of that for \mathcal{L} , adding significant overhead [33]. In an alternative approach [33], instead of variationally searching for the local MPS, one can solve the zero eigenvector for the local effective Lindbladian \mathcal{L}_i obtained by contracting all indices for $\langle\langle \rho | \mathcal{L} | \rho \rangle\rangle$, except those for a single site i , so that sites $j \neq i$ form an environment for site i .

Here we adapt this approach directly to the frequency-space representation of ρ and $\hat{\mathcal{L}}$, seeking to approximately prepare the NESS satisfying $\hat{\mathcal{L}}_i^{nm} |\rho^m\rangle\rangle = 0$ by sweeping through a sequence of local eigenvalue problems for $M_{\mu_i}^m$ (see Fig. 1), using an implicitly restarted Arnoldi method based non-Hermitian eigensolver implemented in the ARPACK library [37]. Working in frequency-space requires imposing additional constraints on the solutions. Physical states satisfy $\text{Tr} \rho(t) = \langle\langle \mathbb{I} | \rho(t) \rangle\rangle = 1 \forall t$, which demands $\text{Tr} \rho^n = \langle\langle \mathbb{I} | \rho^n \rangle\rangle = \delta_{n0}$ where $\langle\langle \mathbb{I} \rangle\rangle$ is the maximally mixed state. We enforce this condition by penalizing violations by modifying how the extended Lindbladian acts on vectors as $\hat{\mathcal{L}} \rightarrow \hat{\mathcal{L}}'$ with:

$$\begin{aligned} \hat{\mathcal{L}}'^{nm} |\rho^m\rangle\rangle &= (\hat{\mathcal{L}}^{nm} - P_0 \langle\langle \mathbb{I} \rangle\rangle \langle\langle \mathbb{I} | (1 - \delta_{n0}) \delta_{nm} \rangle\rangle) |\rho^m\rangle\rangle \\ &\quad - P_1 \exp(-|\text{Tr} \rho^n|^2 / \delta^2) |\rho^n\rangle\rangle, \end{aligned} \quad (5)$$

where P_0, P_1, δ are penalty parameters. In practice, we start with several warm-up sweeps with proper penalty parameters ($P_0 = P_1 = 1000$ and $\delta = 0.01$ in our implementation) to avoid local minima violating the trace constraint, and then remove the penalty for further DMRG sweeping. (See Appendix B and C for discussion on convergence and positivity of density matrices)

Dynamical approach to the NESS – The MPO-based method can be naturally extended to solve long-lived decaying modes of Floquet Lindbladian, with $\text{Re} \lambda > 0$, by a similar approach to excited state DMRG [38]. To explore this, we first review some basic properties of the (extended) Lindbladian: (i) the Lindbladian has a bi-orthonormal basis, where left and right eigenvectors are defined by $\hat{\mathcal{L}} |\rho_\alpha^R\rangle\rangle = \lambda_\alpha |\rho_\alpha^R\rangle\rangle$ and $\hat{\mathcal{L}}^\dagger |\rho_\alpha^L\rangle\rangle = \lambda_\alpha^* |\rho_\alpha^L\rangle\rangle$ and satisfy the orthogonal relations $\langle\langle \rho_\alpha^L | \rho_\beta^R \rangle\rangle = \delta_{\alpha\beta}$; (ii) The corresponding eigenvalues $\{\lambda_{\alpha=0,1,\dots}\}$ can be sorted as $0 = \lambda_0 > \text{Re} \lambda_1 \geq \text{Re} \lambda_2 \geq \dots$ (we assume that the zero eigenvalue is not degenerate in the following discussion). In particular $|\rho_0^L\rangle\rangle = \langle\langle \mathbb{I} \rangle\rangle$ due to the trace preservation of Lindblad operator; (iii) The complex eigenvalues must occur in a pair of complex conjugate since when ρ is an eigenvector, ρ^\dagger is also an eigenvector.

Based on properties of the Lindbladian and in analogy to the Hamiltonian case [38], one can define $\hat{\mathcal{L}}_1 = \hat{\mathcal{L}} - w \langle\langle \mathbb{I} \rangle\rangle \langle\langle \mathbb{I} | (\hat{\mathcal{L}}_1^\dagger = \hat{\mathcal{L}}^\dagger - w |\rho_{ss}\rangle\rangle \langle\langle \rho_{ss} |)$ where w is the penalty energy for the vector not orthogonal to the zeroth left (right) eigenvector. For large enough w , the solved eigenvalue with largest real part will give the first right (left)

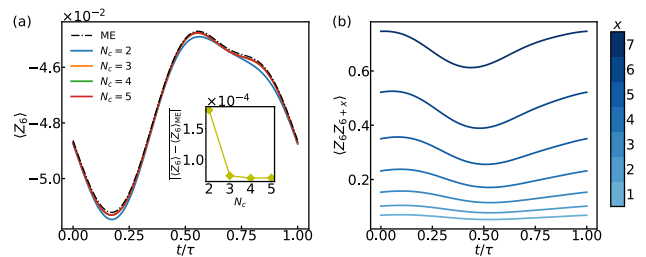


FIG. 2. **NESS of driven-dissipative Ising chain** – with $(J, h, g, \gamma, \omega) = (1.0, 0.5, 1.0, 1.0, 5.0)$. (a) Time-dependent expectation values of magnetization $\langle Z_6 \rangle$ for a system size $L = 11$, with $\chi = 36$, compared with the master equation evolution result. The period-averaged error (inset) decays rapidly with N_c to the numerical accuracy of the eigensolver. (b) Spatial correlations $\langle Z_6 Z_{6+x} \rangle$ for a larger chain with $L = 21$, using $(N_c, \chi) = (4, 20)$.

eigenvector $|\rho_1^R\rangle\rangle$ ($|\rho_1^L\rangle\rangle$). In principle, this procedure can be done recursively to the n^{th} eigenvector by adding n projectors, however for the pair of eigenvectors whose eigenvalues are in complex conjugate pairs $\lambda = a \pm ib$, they cannot be distinguished by their real part. Thus, we focus only on the first decaying mode by targeting the largest real part of eigenvalues, which dominates the approach to the steady state at long times.

Benchmark: driven-dissipative Ising chain – We first benchmark our OFDMRG method in a driven-dissipative Ising model on a length L spin-1/2 chain with Pauli operators $\{X_i, Y_i, Z_i\}$ for sites $i = 1 \dots L$ with Hamiltonian:

$$H(t) = \sum_i [p(t) (-J Z_i Z_{i+1} + h Z_i) + q(t) g X_i], \quad (6)$$

where $p(t) = (1 - \sin \omega t)/2$, $q(t) = (1 + \sin \omega t)/2$, and time-independent majority-rule jump operators

$$L_i = \sqrt{\gamma} (2 | \uparrow \uparrow \uparrow \rangle \langle \uparrow \downarrow \uparrow | + | \uparrow \uparrow \downarrow \rangle \langle \uparrow \downarrow \downarrow | + | \uparrow \downarrow \downarrow \rangle \langle \uparrow \downarrow \downarrow | + | \uparrow \downarrow \uparrow \downarrow \rangle \langle \uparrow \downarrow \uparrow \downarrow |). \quad (7)$$

To compare our method with the exact evolution of Lindblad master equation implemented in QUTIP [39], we simulate a chain with array length $L = 11$. We find excellent convergence in the central magnetization $\langle Z_6 \rangle$ to the exact solution with increasing frequency-space cutoff N_c , achieving residual error $\sim 10^{-4}$ for $N_c \sim 5$ that is consistent with residual error in the zero-eigenvalue solver of OFDMRG and the order of magnitude of Schmidt components at the bond-dimension cutoff (See Appendix B). The OFDMRG method also extends straightforwardly to larger systems with polynomial-in- L scaling. For example, in Fig. 2 we show spatial correlations for a size $L = 21$, which would require enormous computational resources to compute exactly.

Dissipatively-stabilizing a discrete time-crystal (DTC) – Having benchmarked the performance of the OFDMRG approach, we now turn to the question of

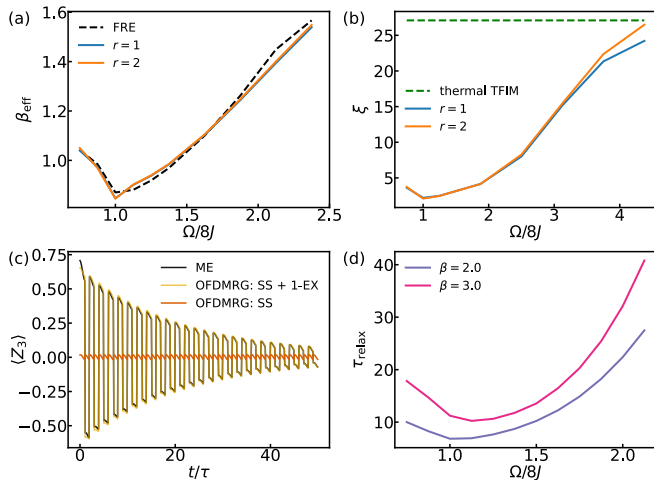


FIG. 3. **OFDMRG for dissipative DTC model** Eq. 8 for $J = 1$, $h = 0.5$, $\omega_c = 2$, and unless otherwise specified: $\beta = 2$ and $r = 2$. (a) Comparison between effective temperature β_{eff} of the dissipative DTC model calculated by OFDMRG method and that from solving FRE, with $L = 11$, $g = 0.05$, $\gamma = 0.2$, and $(N_c, \chi) = (1, 16)$. (b) Correlation lengths ξ of the dissipative DTC model for $L = 31$, $g = 0.05$, $\gamma = 0.2$, and $(N_c, \chi) = (1, 8)$. The correlation length for a thermal state of transverse-field Ising model (TFIM) with $\beta = 2$ is given as a reference. (c) Comparison between transient dynamics of $\langle Z_3 \rangle$ calculated by OFDMRG method and by the exact evolution of master equation (ME) for $L = 5$, $g = 0.2$, $\gamma = 2$, $\beta = 5$, high-frequency ($\Omega = 10$), and $(N_c, \chi) = (2, 16)$. (d) Relaxation time of the dissipative DTC model for $L = 21$, $g = 0.2$, $\gamma = 2$, and $(N_c, \chi) = (1, 16)$.

whether a pre-thermal dynamical phase can be stabilized by coupling to a cold bath. As an example, we study a model for a pre-thermal DTC model [11] coupled to a thermal bath. For the system part, we consider one-dimensional Ising model driven by periodic π -pulses with generic perturbation breaking the \mathbb{Z}_2 symmetry, which serves as a prototypical model for the pre-thermal DTC [11]

$$H(t) = \sum_i \left[\frac{\pi}{2} \sum_n \delta(t - n\tau) X_i - JZ_i Z_{i+1} + hZ_i f(t) + gX_i \right], \quad (8)$$

where $f(t) = (1 - \cos \Omega t)$. Various disordered and/or long-range interacting incarnations of this Hamiltonian have been studied in previous theoretical studies and implemented experimentally in a variety of systems [2, 3] to study MBL and prethermal mechanisms for stabilizing DTC order in (approximately) closed systems.

Here, we introduce dissipation by coupling each spin, via coupling strength γ , to a separate ohmic bath with spectral function $J(\varepsilon) = \frac{\varepsilon}{\varepsilon_0} e^{-|\varepsilon|/\omega_c} / (1 - e^{-\beta\varepsilon})$, where $\beta = 1/T$ is the inverse temperature of the bath, ε_0 is a characteristic energy scale, and ω_c is the local bandwidth of the bath, which will play an important role in controlling

the steady state [40]. We compute the effective time-dependent jump operators for this model using a Born-Markov approximation (see Appendix D for details), and then truncate these to a finite range of $(2r + 1)$ sites to incorporate into the OFDMRG procedure.

The singular δ -train has unbounded Fourier spectrum, which would be long range in frequency-space. However, for models with smooth $f(t)$ satisfying $f(0) = 0$, we can cure this by transforming into a rotating frame of the δ -function X_π -pulses. In the rotating frame the periodicity is doubled to 2τ , but there is a dynamical symmetry: $H(t + \tau) = XH(t)X$ with $X = \prod_i X_i$. In the DTC phase [2, 3], this dynamical symmetry is spontaneously broken, resulting in persistent period-doubled oscillations, and manifesting in long-range mutual information between distant spins [41]. Unlike the long-range interacting pre-thermal DTC model realized recently in trapped-ion experiments [42] such spontaneous symmetry breaking is forbidden in any short-range interacting $1d$ system that thermalizes to a finite temperature. Instead, one expects the length- and time-scales for these signatures to diverge if the system is successfully cooled to a pre-thermal ground-state. The criterion of cooling near the pre-thermal ground is also required to realize dynamical Floquet topological phases (in any dimension), whose properties rely crucially on quantum coherence and entanglement.

Our goal is to assess whether and under what conditions the resulting NESS resembles a low-temperature Floquet Gibbs state with extended range DTC correlations. To this end, we compute (i) the NESS entropy $S_{\text{ss}} = -\text{Tr}(\rho_{\text{ss}} \log \rho_{\text{ss}})$; (ii) the NESS DTC spatial correlation length ξ defined by fitting the averaged correlation function $\langle Z_{j+x} Z_j \rangle$ to the form $e^{-x/\xi}$ (shown in Fig. 3(a)(b)). The NESS results are compared to properties of a thermal state $\rho_{\text{thermal}} = \frac{1}{\mathcal{Z}} e^{-\beta D}$ where D is the effective Floquet Hamiltonian obtained by performing a high-frequency (ven Vleck) expansion to the second order. We can extract an effective inverse temperature $\beta_{\text{eff}} = 1/T_{\text{eff}}$ by comparing the system entropy S_{ss} to the thermal entropy of D . D takes the form of a transverse-field Ising model with ordered ground-state, and the characteristic energy scale to make a local spin-flip excitation of D is $4J$, which will result enhanced drive-induced heating when $\Omega/2 \approx 4J$, resulting in enhanced T_{eff} . We also compare results to solutions to an approximate Floquet rate equation (FRE) [22, 43, 44] (for $L = 11$) obtained from a Fermi-Golden rule treatment bath-induced transition rates between eigenstates of the effective system Hamiltonian D in a rotating frame, which neglects off-diagonal coherences in the system density matrix (See details in Appendix E). As driving frequency increases beyond $8J$, this heating is suppressed, and the system's β_{eff} asymptotes to that of the bath (note that, simulating colder temperatures requires keeping a larger spatial

extent, r , to the ab initio computed jump operators), and ξ increases towards the thermal correlation length of ρ_{thermal} at the bath temperature. Importantly, the Floquet Gibbs state arises only when the local bath bandwidth satisfies $\omega_c \ll |\frac{\Omega}{2} - 4J|$, so that bath-assisted drive-induced heat absorption processes are suppressed (See details in Appendix E).

We further explore the long-time DTC dynamics, through asymptotic decay rate $\tau_{\text{relax}} = -(\text{Re}\lambda_1)^{-1}$ of period doubled oscillations obtained by computing the first excited eigenstate $|\rho_1\rangle$, as well as the explicit dynamics of $\langle Z_j(t) \rangle$ for the $|\rho(t)\rangle = |\rho_{\text{ss}}\rangle + e^{-\lambda_1 t} \langle \rho_I | \rho_1 \rangle |\rho_1\rangle$, which captures the long-time dynamics from an initial product state: $\rho_I = \prod_i (\sin \frac{\pi}{8} | \uparrow \rangle + \cos(\frac{\pi}{8}) | \downarrow \rangle) (\sin \frac{\pi}{8} \langle \uparrow | + \cos(\frac{\pi}{8}) \langle \downarrow |)$. As shown in Fig. 3(c), the dynamical results are compared against exact master equation simulations (for $L = 5$, close to the limit of a single workstation). We observe quantitative agreement between the time-dependent dynamics of the excited-state OFDMRG method with the master equation simulations, confirming that the long-time dynamics is indeed dominated by the first decaying mode. Further, in Fig. 3(d), we observe that the DTC time scale increases with driving frequency Ω (for $\Omega/2 > 4J$), asymptoting to a finite time-scale that increases as the bath is cooled.

Discussion and outlook – These results confirm the expectation that there is a parameter regime of large

driving frequency ($\Omega \gg 8J$), moderate bath bandwidth ($\omega_c \ll |\frac{\Omega}{2} - 4J|$), and moderately-weak system bath coupling ($e^{-J/\Omega} \ll \gamma \ll J$) where coupling the pre-thermal DTC model to a bath successfully produces a Floquet Gibbs-like state with temperature close to that of the bath (See details in Appendix E and F). Further, the OFDMRG method successfully captures this behavior in system sizes that greatly exceed those accessible by exact master equation simulations (here we simulated up to $L = 31$ on a single computer, which would be limited to $L \lesssim 6$ for exact computation).

We expect this technique to be useful in designing realistic realizations of dissipatively-stabilized dynamical phases in solid-state devices and atomic physics quantum simulators. The OFDMRG also permits a controlled means to assess the validity of various approximation methods such as Floquet rate equations which could potentially be used beyond $1d$. Natural future targets for extending the OFDMRG method include studying NESS of quasiperiodically driven systems [45–47] (with multiple frequency-space directions), and incorporating non-Markovian effects [48, 49].

Acknowledgments We thank Brayden Ware and Romain Vasseur for insightful discussions. This work was supported by NSF DMR-1653007 and the Alfred P. Sloan Foundation through a Sloan Research Fellowship (A.C.P.).

-
- [1] Takashi Oka and Sota Kitamura, “Floquet Engineering of Quantum Materials,” Annual Review of Condensed Matter Physics **10**, 1–22 (2018).
 - [2] Fenner Harper, Rahul Roy, Mark S Rudner, and SL Sondhi, “Topology and broken symmetry in floquet systems,” arXiv preprint arXiv:1905.01317 (2019).
 - [3] Dominic V. Else, Christopher Monroe, Chetan Nayak, and Norman Y. Yao, “Discrete Time Crystals,” Annual Review of Condensed Matter Physics **11**, 467–499 (2020).
 - [4] Luca D’Alessio and Marcos Rigol, “Long-time Behavior of Isolated Periodically Driven Interacting Lattice Systems,” Physical Review X **4**, 041048 (2014).
 - [5] Achilleas Lazarides, Arnab Das, and Roderich Moessner, “Equilibrium states of generic quantum systems subject to periodic driving,” Physical Review E **90**, 012110 (2014).
 - [6] Achilleas Lazarides, Arnab Das, and Roderich Moessner, “Fate of Many-Body Localization Under Periodic Driving,” Physical Review Letters **115**, 030402 (2015).
 - [7] Dmitry A. Abanin, Wojciech De Roeck, and François Huveneers, “Exponentially Slow Heating in Periodically Driven Many-Body Systems,” Physical Review Letters **115**, 256803 (2015).
 - [8] Dmitry A. Abanin, Wojciech De Roeck, Wen Wei Ho, and François Huveneers, “Effective Hamiltonians, prethermalization, and slow energy absorption in periodically driven many-body systems,” Physical Review B **95**, 014112 (2017).
 - [9] Dmitry Abanin, Wojciech De Roeck, Wen Wei Ho, and François Huveneers, “A Rigorous Theory of Many-Body Prethermalization for Periodically Driven and Closed Quantum Systems,” Communications in Mathematical Physics **354**, 809–827 (2017).
 - [10] Marin Bukov, Luca D’Alessio, and Anatoli Polkovnikov, “Universal high-frequency behavior of periodically driven systems: from dynamical stabilization to Floquet engineering,” Advances in Physics **64**, 139–226 (2015).
 - [11] Dominic V. Else, Bela Bauer, and Chetan Nayak, “Prethermal Phases of Matter Protected by Time-Translation Symmetry,” Physical Review X **7**, 011026 (2017).
 - [12] André Eckardt and Egidijus Anisimovas, “High-frequency approximation for periodically driven quantum systems from a Floquet-space perspective,” New Journal of Physics **17**, 093039 (2015).
 - [13] Kaoru Mizuta, Kazuaki Takasan, and Norio Kawakami, “High-frequency expansion for Floquet prethermal phases with emergent symmetries: Application to time crystals and Floquet engineering,” Physical Review B **100**, 020301 (2019).
 - [14] Andrew C Potter and Romain Vasseur, “Symmetry constraints on many-body localization,” Physical Review B **94**, 224206 (2016).
 - [15] Sumilan Banerjee and Ehud Altman, “Variable-range

- hopping through marginally localized phonons,” *Physical Review Letters* **116**, 116601 (2016).
- [16] Wojciech De Roeck and Franois Huveneers, “Stability and instability towards delocalization in many-body localization systems,” *Phys. Rev. B* **95**, 155129 (2017).
- [17] Phillip Weinberg, Marin Bukov, Luca D’Alessio, Anatoli Polkovnikov, Szabolcs Vajna, and Michael Kolodrubetz, “Adiabatic perturbation theory and geometry of periodically-driven systems,” *Physics Reports* **688**, 1–35 (2017), *adiabatic Perturbation Theory and Geometry of Periodically-Driven Systems*.
- [18] Mark S. Rudner and Netanel H. Lindner, “Band structure engineering and non-equilibrium dynamics in Floquet topological insulators,” *Nature Reviews Physics* **2**, 229–244 (2020).
- [19] Farhang Haddadfarshi, Jian Cui, and Florian Mintert, “Completely Positive Approximate Solutions of Driven Open Quantum Systems,” *Physical Review Letters* **114**, 130402 (2015).
- [20] C. M. Dai, Z. C. Shi, and X. X. Yi, “Floquet theorem with open systems and its applications,” *Physical Review A* **93**, 032121 (2016).
- [21] Tatsuhiko N. Ikeda and Masahiro Sato, “General description for nonequilibrium steady states in periodically driven dissipative quantum systems,” *Science Advances* **6**, eabb4019 (2020).
- [22] Tatsuhiko Ikeda, Koki Chinzei, and Masahiro Sato, “Nonequilibrium steady states in the Floquet-Lindblad systems: van Vleck’s high-frequency expansion approach,” *SciPost Physics Core* **4**, 033 (2021).
- [23] Klaus Mølmer, Yvan Castin, and Jean Dalibard, “Monte carlo wave-function method in quantum optics,” *J. Opt. Soc. Am. B* **10**, 524–538 (1993).
- [24] Jean Dalibard, Yvan Castin, and Klaus Mølmer, “Wavefunction approach to dissipative processes in quantum optics,” *Phys. Rev. Lett.* **68**, 580–583 (1992).
- [25] R. Dum, P. Zoller, and H. Ritsch, “Monte carlo simulation of the atomic master equation for spontaneous emission,” *Phys. Rev. A* **45**, 4879–4887 (1992).
- [26] U. Schollwöck, “The density-matrix renormalization group,” *Rev. Mod. Phys.* **77**, 259–315 (2005).
- [27] Michael M. Wolf, Frank Verstraete, Matthew B. Hastings, and J. Ignacio Cirac, “Area laws in quantum systems: Mutual information and correlations,” *Phys. Rev. Lett.* **100**, 070502 (2008).
- [28] F. Verstraete, J. J. García-Ripoll, and J. I. Cirac, “Matrix product density operators: Simulation of finite-temperature and dissipative systems,” *Phys. Rev. Lett.* **93**, 207204 (2004).
- [29] Michael Zwolak and Guifré Vidal, “Mixed-state dynamics in one-dimensional quantum lattice systems: A time-dependent superoperator renormalization algorithm,” *Phys. Rev. Lett.* **93**, 207205 (2004).
- [30] Guifré Vidal, “Efficient simulation of one-dimensional quantum many-body systems,” *Phys. Rev. Lett.* **93**, 040502 (2004).
- [31] Steven R. White and Adrian E. Feiguin, “Real-time evolution using the density matrix renormalization group,” *Phys. Rev. Lett.* **93**, 076401 (2004).
- [32] Jian Cui, J. Ignacio Cirac, and Mari Carmen Bañuls, “Variational Matrix Product Operators for the Steady State of Dissipative Quantum Systems,” *Physical Review Letters* **114**, 220601 (2015).
- [33] Eduardo Mascarenhas, Hugo Flayac, and Vincenzo Savona, “Matrix-product-operator approach to the nonequilibrium steady state of driven-dissipative quantum arrays,” *Physical Review A* **92**, 022116 (2015).
- [34] Hendrik Weimer, Augustine Kshetrimayum, and Román Orús, “Simulation methods for open quantum many-body systems,” *Rev. Mod. Phys.* **93**, 015008 (2021).
- [35] Steven R. White, “Density matrix formulation for quantum renormalization groups,” *Phys. Rev. Lett.* **69**, 2863–2866 (1992).
- [36] Mark S Rudner and Netanel H Lindner, “The floquet engineer’s handbook,” arXiv preprint arXiv:2003.08252 (2020).
- [37] <http://www.caam.rice.edu/software/ARPACK/>.
- [38] E.M. Stoudenmire and Steven R. White, “Studying Two-Dimensional Systems with the Density Matrix Renormalization Group,” *Annual Review of Condensed Matter Physics* **3**, 111–128 (2012).
- [39] J.R. Johansson, P.D. Nation, and Franco Nori, “Qutip 2: A python framework for the dynamics of open quantum systems,” *Computer Physics Communications* **184**, 1234–1240 (2013).
- [40] Karthik I. Seetharam, Charles-Edouard Bardyn, Netanel H. Lindner, Mark S. Rudner, and Gil Refael, “Controlled Population of Floquet-Bloch States via Coupling to Bose and Fermi Baths,” *Physical Review X* **5**, 041050 (2015).
- [41] Dominic V. Else, Bela Bauer, and Chetan Nayak, “Floquet Time Crystals,” *Physical Review Letters* **117**, 090402 (2016).
- [42] Antonis Kyprianidis, Francisco Machado, William Morong, Patrick Becker, Kate S Collins, Dominic V Else, Lei Feng, Paul W Hess, Chetan Nayak, Guido Pagano, *et al.*, “Observation of a prethermal discrete time crystal,” *Science* **372**, 1192–1196 (2021).
- [43] Tatsuhiko Shirai and Takashi Mori, “Thermalization in open many-body systems based on eigenstate thermalization hypothesis,” *Physical Review E* **101**, 042116 (2020).
- [44] Takashi Mori, “Floquet states in open quantum systems,” arXiv preprint arXiv:2203.16358 (2022).
- [45] Philipp T. Dumitrescu, Romain Vasseur, and Andrew C. Potter, “Logarithmically slow relaxation in quasiperiodically driven random spin chains,” *Phys. Rev. Lett.* **120**, 070602 (2018).
- [46] Dominic V. Else, Wen Wei Ho, and Philipp T. Dumitrescu, “Long-lived interacting phases of matter protected by multiple time-translation symmetries in quasiperiodically driven systems,” *Phys. Rev. X* **10**, 021032 (2020).
- [47] Aaron J. Friedman, Brayden Ware, Romain Vasseur, and Andrew C. Potter, “Topological edge modes without symmetry in quasiperiodically driven spin chains,” *Phys. Rev. B* **105**, 115117 (2022).
- [48] Kaoru Mizuta, Kazuaki Takasan, and Norio Kawakami, “Breakdown of markovianity by interactions in stroboscopic floquet-lindblad dynamics under high-frequency drive,” *Phys. Rev. A* **103**, L020202 (2021).
- [49] Alexander Schnell, Sergey Denisov, and André Eckardt, “High-frequency expansions for time-periodic lindblad

- generators,” Phys. Rev. B **104**, 165414 (2021).
- [50] A. H. Werner, D. Jaschke, P. Silvi, M. Kliesch, T. Calarco, J. Eisert, and S. Montangero, “Positive Tensor Network Approach for Simulating Open Quantum Many-Body Systems,” Physical Review Letters **116**, 237201 (2016).
- [51] Heinz-Peter. Breuer and Francesco Petruccione, *The Theory of Open Quantum Systems* (Clarendon, 2002).
- [52] Frederik Nathan and Mark S. Rudner, “Universal Lindblad equation for open quantum systems,” Physical Review B **102**, 115109 (2020).
- [53] Evgeny Mozgunov and Daniel Lidar, “Completely positive master equation for arbitrary driving and small level spacing,” Quantum **4**, 227 (2020).
- [54] Zongping Gong and Ryusuke Hamazaki, “Bounds in nonequilibrium quantum dynamics,” arXiv preprint arXiv:2202.02011 (2022).
- [55] Tatsuhiko Shirai, Juzar Thingna, Takashi Mori, Sergey Denisov, Peter Hänggi, and Seiji Miyashita, “Effective Floquet–Gibbs states for dissipative quantum systems,” New Journal of Physics **18**, 053008 (2016).

A. Floquet theorem for open quantum systems

Consider a time-periodic Liouvillian superoperator

$$\frac{d\rho}{dt} = \mathcal{L}(t)[\rho]. \quad (\text{A1})$$

By integrating both sides, one can define a time evolution superoperator

$$\mathcal{E}(t, t_0) = \mathcal{T} \exp\left(\int_{t_0}^t ds \mathcal{L}(s)\right), \quad (\text{A2})$$

with

$$\rho(t) = \mathcal{E}(t, t_0)[\rho(t_0)]. \quad (\text{A3})$$

For general initial and final time, one can always decompose the evolution as multiple one-period evolution and some in-period evolution

$$\mathcal{E}(t_f, t_0) = \mathcal{E}(t + n\tau, t_0) = \mathcal{E}(t, t_0)\mathcal{E}(t_0 + \tau, t_0)^n, \quad (\text{A4})$$

where $t \in [t_0, t_0 + \tau]$. Here the one-period evolution superoperator $\mathcal{E}(t_0 + \tau, t_0)$ is of particular interest.

One can obtain a complete basis $\{\rho_\alpha(t_0)\}$ of density matrix by diagonalizing the one-period evolution superoperator at t_0

$$\mathcal{E}(t_0 + \tau, t_0)[\rho_\alpha(t_0)] = e^{-\lambda_\alpha \tau} \rho_\alpha(t_0). \quad (\text{A5})$$

The eigenstates at arbitrary time t with the same spectrum are given by $\rho_\alpha(t) = \mathcal{E}(t, t_0)\rho_\alpha(t_0)$:

$$\mathcal{E}(t + \tau, t)[\rho_\alpha(t)] = \mathcal{E}(t, t_0)\mathcal{E}(t_0 + \tau, t_0)\mathcal{E}(t_0, t)[\rho_\alpha(t)] = \mathcal{E}(t, t_0)\mathcal{E}(t_0 + \tau, t_0)[\rho_\alpha(t_0)] = e^{-\lambda_\alpha \tau} \rho_\alpha(t). \quad (\text{A6})$$

Analogous to the Bloch state, each eigenstate satisfying $\rho_\alpha(t + \tau) = e^{-\lambda_\alpha \tau} \rho_\alpha(t)$ can be decomposed as

$$\rho_\alpha(t) = e^{-\lambda_\alpha t} \tilde{\rho}_\alpha(t), \quad (\text{A7})$$

where $\tilde{\rho}_\alpha(t) = \tilde{\rho}_\alpha(t + \tau)$. Importantly, one can thus expand $\tilde{\rho}_\alpha(t)$ into Fourier series

$$\tilde{\rho}_\alpha(t) = \sum_n e^{in\Omega t} \rho_\alpha^n, \quad (\text{A8})$$

which allows one to solve the time-periodic Liouvillian as a time-independent problem in an extended Hilbert space $\mathcal{H}^2 \times \mathbb{Z}$ with basis ρ_α^n .

B. OFDMRG Implementation Details: Preconditioning heuristics and convergence checks

Besides adding penalizing terms to meet the trace constraints, in the implementation, we also use some warm-up steps to avoid getting stuck in local minima: (i) solve $N_c = 0$ first, i.e. time-averaged Lindbladian as a initial guess

and then gradually increase N_c until get converged result; (ii) gradually increase the bond dimension of the MPO to obtain good convergence; (iii) For the weak dissipation case, i.e. $\gamma \sim |L_\alpha|^2$ is small, the dissipative gap is usually even smaller than the spectral gap of Hamiltonian, and then it is easy to become trapped by a local minima. To overcome this, we start with a large $\gamma \sim 1$ and decrease it gradually.

As mentioned in the main text, the numerical error of our method arises from cut-offs in the frequency-space and the MPO bond dimension. The error from the frequency-space truncation is controlled by $|\rho^{N_c}|/|\rho^0|$. In Fig. 4(a) we can see $|\rho^n|/|\rho^0|$ decays exponentially in $|n|$ away from $n = 0$, indicating localization in frequency-space compatible with truncation to finite $|n| < N_c$. Fig. 4(b) shows the exponential decaying of Schmidt components in the MPO ansatz, which allows the large system size calculation. In practice, we set 10^{-3} as a tolerance bar for determining if the calculation is converged.

C. Positivity of density matrices

Besides having unit trace, a physical density matrix must also satisfy a positivity condition, which ensures the positive occupation on each eigenstate, this condition is generally NP-hard (in system size) problem to even check. In our algorithm, the positivity of density matrix is not manifestly guaranteed (compared to the local purified tensor network ansatz [50]). However, as the extended Lindbladian is a complete positive superoperator, the exact steady-state solution is a positive fixed point and thus if our procedure does not become stuck in any local minima, and if there is no other dark state solution, we expect the solved density matrix is positive at least up to the numerical error from frequency-space and bond-dimension truncation. Although the direct check on the positivity is NP-hard, we provide an indirect check on the non-Hermiticity $|\rho^n - \rho^{\dagger, -n}|/|\rho^0|$ as shown in Fig. 4(c). We observe the non-Hermiticity of density matrix is small and consistent with error induced by truncations on the frequency-space and bond dimension, which is at the same order of $\sigma^n(\chi)|\rho^n|/|\rho^0|$. Besides, all the physical observables we demonstrated in the main text take physical values with tolerance set by truncation errors.

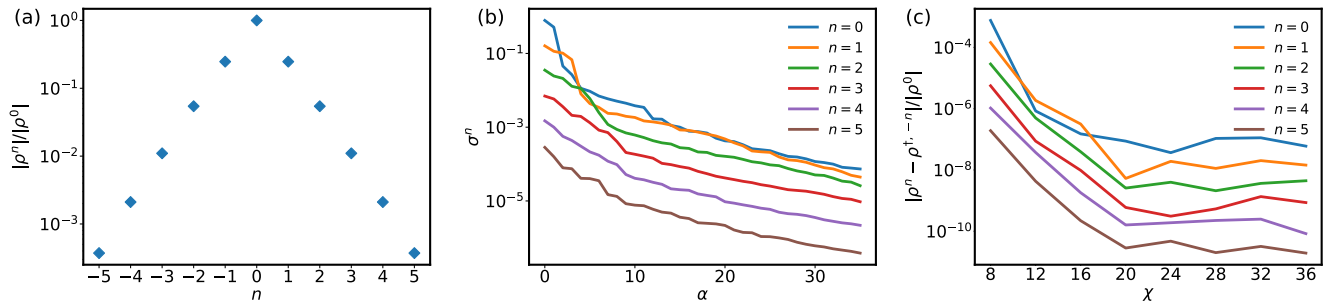


FIG. 4. **Convergence and positivity of density matrices** – (a) The relative weight $\frac{|\rho^n|}{|\rho^0|}$ for each Fourier component n of Floquet density matrix for $N_c = 5$ and $\chi = 36$. (b) Schimt components σ^n for each Fourier component n of Floquet density matrix for $N_c = 5$ and $\chi = 36$. (c) Non-Hermiticity $\frac{|\rho^n - \rho^{\dagger, -n}|}{|\rho^0|}$ for each Fourier component n of Floquet density matrix versus χ .

D. General jump operators from microscopic model and MPO construction for dissipative discrete time-crystal model

In the driven-dissipative Ising model, we studied a phenomenological Lindbladian. However, to realistically capture the interactions between a system and a thermal bath at a specific temperature, one must microscopically derive the resulting master equation. The most commonly presented derivations of the Lindblad master equations [51] are usually based on two main approximations: (i) the Born-Markov approximation (BMA), which requires the bath remains in approximate equilibrium while the system is dissipating, that is $\tau_R \gg \tau_B$ where $\tau_R \sim \gamma^{-1}$ is the relaxation time from system to bath and τ_B is the bath correlation time; and (ii) the rotating wave approximation (RWA) requiring the intrinsic time scale of the system $\tau_X \sim |\varepsilon_i - \varepsilon_j|^{-1}$ is small compared to the relaxation time, so that the oscillation between system energy levels can be smeared out within the relaxation process. The BMA is valid for weak system-bath coupling and Markovian baths (the latter condition is independent of the system). However, the RWA is usually broken down in quantum many-body systems, where the level spacing goes to infinite small in the

thermodynamic limit. Recently, some important progresses have been made to derive the Lindblad master equation without the RWA and its error bound is consistent with the BMA only[52, 53]. Here we leverage the Lindblad equation derivation from Ref [52] to describe the Floquet-dissipative system of interest.

Consider a system-plus-bath Hamiltonian $H(t) = H_S(t) + H_B + H_{SB}$, where $H_S(t)$ is the Hamiltonian for the system, including periodic driving, H_B is for the thermal bath, and H_{SB} represents the system-bath interactions, which can be generally decomposed as

$$H_{SB} = \sum_i \sqrt{\gamma} \mathcal{X}_i \otimes B_i, \quad (\text{D1})$$

where γ is a parameter representing the strength of system-bath coupling, operator \mathcal{X}_i acts only on the system, and operator B_i acts only on the bath. Note that the behavior of bath is characterized completely by the bath correlation function $J_{ij}(t-s) = \langle B_i(t) B_j(s) \rangle$ and the corresponding spectral density $J_{ij}(\omega) = \int dt J_{ij}(t) e^{i\omega t}$. As shown in Ref.[52], a universal Lindblad master equation can be derived up to the accuracy of the BMA, i.e. $\mathcal{O}(\gamma^2 \tau_B)$:

$$\mathcal{L}(t)[\rho] = -i[H(t) + \Lambda(t), \rho] + \sum_i \left(L_i(t) \rho L_i^\dagger(t) - \frac{1}{2} \{L_i^\dagger(t) L_i(t), \rho\} \right), \quad (\text{D2})$$

with the Lamb shift $\Lambda(t)$ and jump operators given by:

$$\Lambda(t) = \sum_i \frac{\gamma}{2i} \int_{-\infty}^{\infty} ds ds' U(t, s) \mathcal{X}_i U(s, s') \mathcal{X}_i U(s', t) \phi(s-t, s'-t), \quad (\text{D3})$$

$$L_i(t) = \sqrt{\gamma} \int_{-\infty}^{\infty} ds g(s-t) U(t, s) \mathcal{X}_i U(s, t), \quad (\text{D4})$$

where $U(t, s) = \mathcal{T} \exp\left(-i \int_s^t dt' H(t')\right)$ is the time evolution operator for the system, $\phi(t, s) = g(t)g(-s)\text{sgn}(t-s)$ and $g(s)$ is the jump correlator given by the Fourier transformation of the squared root of the bath spectral density $J(\omega)$

$$g(t) = \frac{1}{2\pi} \int_{-\infty}^{\infty} d\omega g(\omega) e^{-i\omega t}, \quad g(\omega) = \sqrt{J(\omega)}, \quad (\text{D5})$$

Note that in the weak coupling limit, the Lamb shift does not significantly change the NESS, thus we neglect the Lamb shift in our discussion, however $\Lambda(t)$ could be straightforwardly incorporated into $H(t)$ if desired.

For specificity, we consider the dissipative DTC mentioned in the main text Eq. 8, coupled to independent thermal baths by $\sqrt{\gamma} \mathcal{X}_i \otimes B_i$, and the bath spectral function is of Ohmic form $J(\varepsilon) = \frac{\varepsilon}{\varepsilon_0} e^{-|\varepsilon|/\omega_c} / (1 - e^{-\beta\varepsilon})$. In the rotating frame of the X_π -pulses, the DTC Hamiltonian (Eq. 8) and jump operators for the universal Lindblad equation read:

$$\tilde{H}(t) = \sum_i \left[-J Z_i Z_{i+1} + g X_i + h Z_i f(t) (-1)^{1+[t/T]} \right], \quad (\text{D6})$$

and

$$\tilde{L}_i(t) = \sqrt{\gamma} \int_{-\infty}^{\infty} ds g(s-t) \tilde{U}(t, s) X_i \tilde{U}(s, t), \quad (\text{D7})$$

where $\tilde{U}(t, s) = \mathcal{T} \exp\left(-i \int_s^t dt' \tilde{H}(t')\right)$ is time-evolution operator for the Hamiltonian in the rotating frame.

In general, jump operators given in Eq.(D7) are not strictly local, but however, have exponential decaying tails out to larger distances. In our implementation we truncate these tails outside a region, $[i-r, i+r]$:

$$\tilde{L}_{i,r}(t) = \sqrt{\gamma} \int_{-\infty}^{\infty} ds g(s-t) \tilde{U}_r(t, s) X_i \tilde{U}_r(s, t), \quad (\text{D8})$$

with $\tilde{U}_r(t, s) = \mathcal{T} \exp\left(-i \int_s^t dt' \tilde{H}_r(t')\right)$ and \tilde{H}_r is only defined in $[i-r, i+r]$. An error bound for such a local truncation on the jump operator is given by considering the Lieb-Robinson bound from cutting the exponential tail outside the light cone of system time-evolution (See Appendix D 1 for the derivation):

$$\|\tilde{L}_i(t) - \tilde{L}_{i,r}(t)\| \lesssim C e^{-\kappa(r-v\tau_B)}, \quad (\text{D9})$$

where C is a non-universal constant, τ_B is the bath correlation time, and v and κ depend only on the system Hamiltonian. For the DTC model, $v \sim 2J$ and $\kappa \sim \log|J/g|$, the truncation is valid when $r \gg 1/\log|J/g| + 2J\tau_B$, which requires small transverse field and bath correlation time. On the other hand, since the bond dimension of a generic MPO representation for superoperators grows exponentially with the active range as $\chi_O = 16^r$, this translates to an exponential growth of computational complexity with the bath correlation time τ_B . In practice we are unable to perform computations with $r \geq 3$, and consider only $r = 1$ and $r = 2$ cases in our implementation. Yet, this range is sufficient to accurately capture the behavior of moderately-low temperature baths ($\beta \lesssim \frac{\pi}{J}$, as lower temperature results in long bath correlations) and for moderately small transverse fields (as large transverse fields result in large v).

Since we are particularly interested in the high-frequency regime (possibly in an appropriately rotating frame), where driving-induced heating is much larger than the relaxation time from the system-bath coupling $\sim \gamma^{-1}$, we adopt a high-frequency expansion to simplify Eq.(D8) as:

$$\tilde{U}_r(t, s) \approx e^{-iK_r(t)} e^{-iD_r(t-s)} e^{iK_r(s)}, \quad (\text{D10})$$

where D_r is the time-independent effective Hamiltonian and the $K_r(t)$ is the periodic kicking operator. (In our implementation we keep the expansion upto $\mathcal{O}(\Omega^{-2})$). A significant advantage of the high-frequency expansion is that we obtain a spectral representation of the jump operators with respect to eigenbasis of the time-independent Floquet Hamiltonian D_r . Define the transformed jump operator $M_{i,r}(t)$ in the interacting frame or the kicking operator $e^{-iK_r(t)}$ as

$$\begin{aligned} M_{i,r}(t) &\approx e^{iK_r(t)} \tilde{L}_{i,r}(t) e^{-iK_r(t)} \\ &= \sqrt{\gamma} \int_{-\infty}^{\infty} ds g(s-t) e^{-iD_r(t-s)} \tilde{\mathcal{Y}}_i(s) e^{iD_r(t-s)} \\ &= \sqrt{\gamma} \sum_k e^{ik\omega t/2} \sum_{mn} g\left(\tilde{\epsilon}_n - \tilde{\epsilon}_m - \frac{k\Omega}{2}\right) \tilde{\mathcal{Y}}_{i,mn}|m\rangle\langle n|, \end{aligned} \quad (\text{D11})$$

where $\tilde{\epsilon}_n$ is the spectrum of D_r and $\tilde{\mathcal{Y}}_i(s) = e^{iK_r(s)} X_i e^{-iK_r(s)}$. Then the approximated jump operator in the rotating frame of the X_π -pulse, $\tilde{L}_{i,r}(t) \approx e^{-iK_r(t)} M_{i,r}(t) e^{iK_r(t)}$, from Eq.(D11) gives a strictly-local operator which is compatible with our MPO-based algorithm.

1. Error bound for the local truncation on jump operators

We next bound the error due to truncating the jump operators to a finite spatial region. Recall that the general jump operator is given by a convolution between jump correlation function $g(t)$ and system-bath interaction operator \mathcal{X}_i

$$L_i(t) = \sqrt{\gamma} \int_{-\infty}^{\infty} ds g(s-t) U(t, s) \mathcal{X}_i(s) U(s, t), \quad U(t, s) = \mathcal{T} \exp\left(-i \int_s^t dt' H(t')\right), \quad (\text{D12})$$

whose effective range is determined by the bath correlation time encoded in $g(t)$ and the Lieb-Robinson bound of the system.

For simplicity, we assume the system-bath interaction operator \mathcal{X}_i only acts on i site and the system Hamiltonian is nearest-neighbor interacting, $H(t) = \sum_j h_{j,j+1}(t)$. Then we follow the procedure in Ref.[54] by considering a modified Hamiltonian with two cut bonds $H_r = H - h_{i-r-1,i-r} - h_{i+r,i+r+1}$. Since H is nearest-neighbor interacting, the support of operators in $[i-r, i+r]$ evolved by H_r is confined in the region $[i-r, i+r]$, which gives a local truncation on jump operators. The corresponding error from replacing H with H_r is given by

$$\begin{aligned} \|L_i(t) - L_{i,r}(t)\| &\leq \sqrt{\gamma} \int_{-\infty}^{\infty} ds g(s-t) \|U(t, s) \mathcal{X}_i(s) U(s, t) - U_r(t, s) \mathcal{X}_i(s) U_r(s, t)\| \\ &= \sqrt{\gamma} \int_{-\infty}^{\infty} ds g(s-t) \| [U_r^\dagger(t, s) U(t, s), \mathcal{X}_i(s)] \| \\ &\leq \sqrt{\gamma} \int_{-\infty}^{\infty} ds g(s-t) \int_s^t dt' \| [V_s(t'), \mathcal{X}_i(s)] \|, \end{aligned} \quad (\text{D13})$$

where

$$V_s(t) = U^\dagger(t, s) (h_{i-r-1,i-r} + h_{i+r,i+r+1}) U(t, s), \quad (\text{D14})$$

is the time-dependent generator of $U^\dagger(t, s)U_r(t, s)$. In the last step, we have invoked the Kubo identity:

$$[A, e^{\beta H}] = \int_0^\beta d\lambda e^{(\beta-\lambda)H} [A, H] e^{\lambda H}. \quad (\text{D15})$$

The general form of the Lieb-Robinson bound is given by

$$\|[\mathcal{O}_X(t), \mathcal{O}_Y]\| \leq C_0 e^{-\kappa S_{XY}} (e^{\kappa v|t|} - 1), \quad (\text{D16})$$

where S_{XY} is minimum distance between operator \mathcal{O}_X and \mathcal{O}_Y , and ξ and v are constants that only depend the system Hamiltonian. Applying the Lieb-Robinson bound to Eq.(D13), we obtain:

$$\|L_i(t) - L_{i,r}(t)\| \leq \sqrt{\gamma} \int_{-\infty}^\infty ds g(s-t) \int_s^t dt' C_0 e^{-\kappa S_{XY}} (e^{\kappa v|t'-s|} - 1) \lesssim C e^{-\kappa(r-v\tau_B)}, \quad (\text{D17})$$

which gives an error bound for replacing $L_i(t)$ by $L_{i,r}(t)$.

E. Floquet rate equation and conditions for Floquet-Gibbs states

When the system-bath coupling γ is significantly smaller than the system characteristic local energy J , a Floquet rate equation (FRE) can be derived from the Floquet Lindblad equation perturbatively[43, 44], by neglecting off-diagonal coherence between Floquet eigenstates (of the system Hamiltonian), and treating only incoherent transitions between different diagonal entries of the density matrix, ρ_{qq} where ε_q is a fixed quasi-energy of the system Hamiltonian with index q . This FRE can be used to obtain intuition about various heating and cooling processes and their associated rates to identify a regime where the system can be effectively cooled into its pre-thermal ground-state.

The steady-state condition for the FRE is:

$$\frac{d\rho_{qq}}{dt} = 0 = \sum_p \rho_{pp} R_{pq} - \rho_{qq} \sum_p R_{qp}, \quad (\text{E1})$$

where the Fermi-Golden rule transition rates are:

$$R_{pq} = \sum_{i,k} J(\varepsilon_q - \varepsilon_p - k\Omega) |\langle p | \mathcal{X}_i^k | q \rangle|^2. \quad (\text{E2})$$

where ε_p and ε_q are quasi-energies of the system Floquet Hamiltonian. Since we are particularly interested in the weak dissipation regime where the BMA holds, it is natural to expect the FLE gives similar results to the FRE. Importantly, the OFDMRG approach can go beyond the FRE, and can also be used to assess the validity of the approximations made in the simpler FRE. In a complementary way, the FRE can be used to gain intuition about the asymptotic behavior observed in the OFDMRG approach.

Specifically, for the dissipative DTC model, we consider the FRE in the X_π -pulse rotating frame and the high-frequency kicking frame:

$$0 = \tilde{\rho}_{qq} \sum_p \tilde{R}_{qp} - \sum_p \tilde{\rho}_{pp} \tilde{R}_{pq}, \quad (\text{E3})$$

$$\tilde{R}_{pq} = \sum_{i,k} J \left(\tilde{\varepsilon}_q - \tilde{\varepsilon}_p - \frac{k}{2}\Omega \right) |\langle p | \tilde{\mathcal{Y}}_i^k | q \rangle|^2. \quad (\text{E4})$$

where $\tilde{\varepsilon}_p$ and $\tilde{\varepsilon}_q$ are replaced by eigenenergies of the effective Hamiltonian D . In practice, we solve Eq.(E3) and Eq.(E4) by the exact diagonalization.

For the static model with $\Omega = 0$, the Fermi-golden-rule like transition rate \tilde{R}_{pq} satisfy the detailed balance condition

$$\frac{\tilde{R}_{pq}}{\tilde{R}_{qp}} = e^{-\beta(\tilde{\varepsilon}_q - \tilde{\varepsilon}_p)}, \quad (\text{E5})$$

with which the rate equation gives to the Gibbs density matrix solution

$$P_p \equiv \rho_{pp} = \frac{e^{-\beta\tilde{\varepsilon}_p}}{Z}, \quad Z \equiv \sum_p e^{-\beta\tilde{\varepsilon}_p}. \quad (\text{E6})$$

For the driven model with $\Omega > 0$, there is driving quanta exchange process given by $J(\tilde{\varepsilon}_q - \tilde{\varepsilon}_p - \frac{k}{2}\Omega)$ terms, which breaks the detailed balance in Eq. E5 and leads to deviations from Gibbs-like solutions for the steady state. When these processes are appreciable, the system steady state typically heats up to a higher effective temperature than the temperature of bath to which it couples. Thus, suppressing the bath-assisted heat absorption requires a small bath spectrum cutoff satisfying [22, 44, 55]

$$J\left(\Lambda - \frac{k}{2}\Omega\right) \sim \exp\left(-\frac{1}{\omega_c}\left|\Lambda - \frac{k}{2}\Omega\right|\right) \ll J(\Lambda), \quad \text{for } k \neq 0, \quad (\text{E7})$$

which is equivalent to

$$\left|\Lambda - \frac{k}{2}\Omega\right| \gg \omega_c, \quad \text{for } k \neq 0, \quad (\text{E8})$$

where Λ is the local energy scale of system, which $\sim 4J$ for the dissipative DTC model. Hence we can conclude that, to realize an approximate Floquet-Gibbs state, the driving frequency Ω needs not only to be larger than the system's energy scale Λ but also must greatly exceed the local bandwidth of bath excitations, ω_c . As one increases the driving frequency, the NESS becomes closer to a Floquet-Gibbs state with the bath temperature (as shown in the main text figures).

F. High-frequency expansion for the system-plus-bath Hamiltonian

In this section, we provide another route to viewing the condition for Floquet-Gibbs states, by applying the high-frequency expansion to the system-plus-bath Hamiltonian and assuming driving frequency Ω is not only larger than the system's energy scale Λ but also the bath spectrum cutoff ω_c , i.e. $\Omega \gg \Lambda$ and $\Omega \gg \omega_c$.

Consider the generic Hamiltonian consisting of system and bath part with periodic external driving

$$H(t) = V(t) + \sqrt{\gamma}X_\alpha(t)B_\alpha + H_B, \quad (\text{F1})$$

where $V(t)$ is the time-periodic Hamiltonian for the system part, X_α and B_α are system-bath interaction operators acting in system and bath Hilbert space respectively, and H_B is the bath Hamiltonian. Here, we do not consider the case where the bath is also driven. In the high-frequency limit, the total evolution can be approximated by the evolution of an effective time-independent Hamiltonian after transforming into a periodically "kicked" frame [11, 13] within a pre-thermal time $t_* = e^{-\mathcal{O}(\Omega/\max\{\omega_c, \Lambda\})}$

$$U(t, s) \approx e^{-iK(t)}e^{-iD(t-s)}e^{iK(s)}, \quad (\text{F2})$$

where D is the effective Hamiltonian and $K(t)$ is the periodic kicking operator. The effective Hamiltonian and kicking operator is given by the van Vleck expansion

$$D = H^0 + \sum_{k \neq 0} \frac{[H^k, H^{-k}]}{2k\Omega} + \sum_{k \neq 0} \frac{[[H^k, H^0], H^{-k}]}{2k^2\Omega^2} + \sum_{k \neq 0} \sum_{q \neq k, 0} \frac{[[H^k, H^{q-k}], H^{-q}]}{3qk\Omega^2} + \mathcal{O}(\Omega^{-3}), \quad (\text{F3})$$

$$iK(t) = \sum_{k \neq 0} \frac{H^k e^{ik\Omega t/2}}{k\Omega} + \sum_{k \neq 0} \frac{[H^k, H^0] e^{ik\Omega t/2}}{k^2\Omega^2} + \sum_{k \neq 0} \sum_{q \neq k, 0} \frac{[H^q, H^{k-q}] e^{ik\Omega t/2}}{2kq\Omega^2} + \mathcal{O}(\Omega^{-3}). \quad (\text{F4})$$

To obtain the effective description of the system degree of freedom which is what we really are interested in, we only keep the first order of $\sqrt{\gamma}$ which is consistent with the Born-Markov approximation we will further apply

$$\begin{aligned} D = & D_V + H_B + \sqrt{\gamma}X^0 B + \sqrt{\gamma} \sum_{k \neq 0} \frac{[X^k, V^{-k}] + [V^k, X^{-k}]}{2k\Omega} B \\ & + \sqrt{\gamma} \sum_{k \neq 0} \frac{[[V^k, X^0], V^{-k}] + [[X^k, V^0], V^{-k}] + [[V^k, V^0], X^{-k}]}{2k^2\Omega^2} B \\ & + \sqrt{\gamma} \sum_{k \neq 0} \frac{[X^k, V^{-k}]}{2k^2\Omega} \frac{[B, H_B]}{\Omega} \\ & + \sqrt{\gamma} \sum_{k \neq 0} \sum_{q \neq k, 0} \frac{[[X^k, V^{q-k}], V^{-q}] + [[V^k, X^{q-k}], V^{-q}] + [[V^k, V^{q-k}], X^{-q}]}{3qk\Omega^2} B \\ & + \mathcal{O}(\Omega^{-3}, \gamma), \end{aligned} \quad (\text{F5})$$

and

$$\begin{aligned}
iK(t) = & iK_V(t) + \sqrt{\gamma} \sum_{k \neq 0} \frac{X^k e^{ik\Omega t/2}}{k\Omega} B \\
& + \sqrt{\gamma} \sum_{k \neq 0} \frac{[V^k, X^0] + [X^k, V^0]}{k^2 \Omega^2} e^{ik\Omega t/2} B + \sqrt{\gamma} \sum_{k \neq 0} \frac{X^k}{k^2 \Omega} e^{ik\Omega t/2} \frac{[B, H_B]}{\Omega} \\
& + \sqrt{\gamma} \sum_{k \neq 0} \sum_{q \neq k, 0} \frac{[X^q, V^{k-q}] + [V^q, X^{k-q}]}{2kq\Omega^2} e^{ik\Omega t/2} B + \mathcal{O}(\Omega^{-3}, \gamma),
\end{aligned} \tag{F6}$$

where D_V and K_V are effective Hamiltonian and kicking operator for the system part, and the summation over α is omitted for simplicity. In general order of inverse frequency, we can group the system-bath coupling part as

$$D = D_V + H_B + \sum_{n=0} \sqrt{\gamma} \frac{Y_n B_n}{\Omega^n} + \mathcal{O}(\gamma), \tag{F7}$$

$$iK(t) = iK_V(t) + \sum_{n=0} \sqrt{\gamma} \frac{Z_n(t) B_n}{\Omega^{n+1}} + \mathcal{O}(\gamma), \tag{F8}$$

where $B_n \equiv \text{ad}_{H_B}^n[B]$ with $\text{ad}_{H_B}[B] \equiv [H_B, B]$ and $|Y_0| \sim |Z_n| \sim \mathcal{O}(1)$, $|Y_{n \geq 1}| \sim \mathcal{O}(\Omega^{-1})$. Notice that the system-bath coupling term includes multiple channels given by different order of comutator with bath Hamiltonian. Then the bath correlation function and spectral density among them are given by $J_{nm}(t-s) \equiv \langle B_n(t) B_m(s) \rangle$ and $J_{nm}(\varepsilon) = \left(\frac{\varepsilon}{\Omega}\right)^{m+n} J(\varepsilon)$. Applying Born-Markov approximation, one can obtain a time-independent Lindblad equation from Eq.(F7)

$$\mathcal{L}_{D_V} \rho = -i[D_V + \Lambda_V, \rho] + \sum_n \left(L_n \rho L_n^\dagger - \frac{1}{2} \{L_n^\dagger L_n, \rho\} \right), \tag{F9}$$

with jump operators given by

$$\begin{aligned}
L_n = & \sqrt{\gamma} \sum_m \int_{-\infty}^{\infty} ds g_{nm}(s-t) e^{-iD_V(t-s)} Y_m e^{iD_V(t-s)} \\
= & \sqrt{\gamma} \sum_m \sum_{ij} g_{nm}(\varepsilon_{ji}) Y_{m,ij} |i\rangle \langle j|,
\end{aligned} \tag{F10}$$

where $g_{nm}(\varepsilon) \sim \left(\frac{\varepsilon}{\Omega}\right)^{m+n} g(\varepsilon)$. Comparing this expression with the transition rate in FRE, detailed balance arises only when g_{00}/J_{00} dominates, and the sub-leading correction occurs at order $\mathcal{O}\left(\frac{g_{01}}{g_{00}}\right) \sim \mathcal{O}\left(\frac{\Lambda}{\Omega}\right)$. Thus with the leading order of jump operators, the steady state ρ_S of the time-independent \mathcal{L}_{D_V} tends to be the thermal state of D_V approximately (ignoring the Lamb shift). Then we check the effect of the periodic kicking from $iK(t)$ also under the Born-Markov approximation. The effective evolution of the system part can be obtained by tracing out the bath degree of freedom

$$\begin{aligned}
\mathcal{E}(t) \rho_S = & \text{Tr}_B \left(e^{-iK(t)} \rho_S \otimes \rho_B e^{iK(t)} \right) \\
= & \text{Tr}_B \left(\rho_S \otimes \rho_B - [iK(t), \rho_S \otimes \rho_B] + \frac{1}{2} [iK(t), [iK(t), \rho_S \otimes \rho_B]] + \mathcal{O}(\Omega^{-3}) \right) \\
= & e^{-iK_V(t)} \rho_S e^{iK_V(t)} + \frac{\gamma}{\Omega^2} \sum_{n,m} [\langle B_n B_m \rangle (Z^n Z^m \rho_S - Z^m \rho_S Z^n) + \langle B_m B_n \rangle (\rho_S Z^m Z^n - Z^n \rho_S Z^m)] + \mathcal{O}(\Omega^{-3}, \gamma^2),
\end{aligned} \tag{F11}$$

where $\langle B_n B_m \rangle \sim \frac{\omega_c^{1+n+m}}{\Omega^{n+m}}$ for a spectral density with exponential cutoff. The first term in Eq. F11 represents the unitary kicking transformation on the system part and the second non-unitary term in Eq. F11 has the order $\mathcal{O}\left(\frac{\gamma \omega_c}{\Omega^2}\right)$, which can be dropped out under the high-frequency limit and weak-dissipation limit. Therefore, we conclude that a Floquet-Gibbs state can be realized when

$$\Omega \gg \{\Lambda, \omega_c\}, \tag{F12}$$

with residual error $\mathcal{O}\left(\frac{\Lambda}{\Omega}\right) + \mathcal{O}\left(\frac{\gamma \omega_c}{\Omega^2}\right)$ for times up to the pre-thermal time $t_* = e^{-\mathcal{O}(\Omega/\max\{\omega_c, \Lambda\})}$, which is consistent with Eq. E8.